Negative Thermal Expansion in Single-Component Systems with Isotropic Interactions†

Mikael C. Rechtsman,‡ Frank H. Stillinger,§ and Salvatore Torquato*,‡,§,||,⊥

Department of Physics, and Department of Chemistry, Princeton University, Princeton, New Jersey 08544, Program in Applied and Computational Mathematics and PRISM, and Princeton Center for Theoretical Physics, Princeton, New Jersey, 08544

Received: August 27, 2007; In Final Form: October 10, 2007

We have devised an isotropic interaction potential that gives rise to negative thermal expansion (NTE) behavior in equilibrium many-particle systems in both two and three dimensions over a wide temperature and pressure range (including zero pressure). An optimization procedure is used in order to find a potential that yields a strong NTE effect. A key feature of the potential that gives rise to this behavior is the softened interior of its basin of attraction. Although such anomalous behavior is well-known in material systems with directional interactions (e.g., zirconium tungstate), to our knowledge, this is the first time that NTE behavior has been established to occur in single-component many-particle systems for isotropic interactions. Using constant-pressure Monte Carlo simulations, we show that as the temperature is increased, the system exhibits negative, zero, and then positive thermal expansion before melting (for both two- and three-dimensional systems). The behavior is explicitly compared to that of a Lennard-Jones system, which exhibits typical expansion upon heating for all temperatures and pressures.

I. Introduction

Control of thermal expansion properties of materials is of technological importance due the need for structures to withstand ambient temperature variations. It is also of fundamental interest because of the variety and intricacy of qualitatively different mechanisms by which materials expand or contract upon heating.[1] In particular, negative thermal expansion (NTE) behavior, a well-known but unusual phenomenon in many-particle systems, has been observed only in multicomponent materials with open unit cell structures in which the bonding of component particles is highly directional. Necessarily a result of anharmonicity of the potential energy of the system, the mechanism by which a material contracts upon heating may be highly intricate.[2]

In the technological realm, materials with zero thermal expansion (those that do not expand or contract upon heating) can aid in the longevity of space structures, bridges, and piping systems.[3] It has been proposed that materials with very large thermal expansion coefficients may function as actuators, and those with negative thermal expansion coefficents may be of use as thermal fasteners.[3]

Perhaps the most common example of a solid exhibiting NTE is that of ice, which contracts upon melting into liquid water.[4] In its solid form, hexagonal ice also undergoes negative thermal expansion for very low temperatures.[1,5] This behavior is a result of the volume dependence of the transverse normal mode (phonon) frequencies of this material, characterized by a negative Grunëisen parameter.[6] Another example of a material that undergoes NTE is zirconium tungstate, ZrW_2O_8, which exhibits this behavior for an extremely large temperature range, namely, 0.3−1050 K.[7] Again, this has been attributed to the phonon properties of the crystal, specifically low-frequency phonon modes that may propagate without distorting the WO_4 tetrahedra and ZrO_6 octahedra that make up the structure.[2] Other examples of materials that exhibit NTE behavior are $Lu_2W_3O_{12}$,[8] diamond and zincblende semiconductors,[9] as well as $Sc_2(WO_4)_3$.[10] An essential feature of the aforementioned systems is their relative openness (low densities) as compared with highly coordinated structures.

Geometries for multicomponent composite systems that give rise to extreme NTE behavior have been designed using topology optimization methods.[3] In these cellular materials, each of three component materials has a nonnegative thermal expansion coefficient, but upon heating, the materials (two solid phases and one void phase) undergo overall contraction. An essential feature of these structures is their local non-convex (re-entrant) "cells". This is an example of an inverse problem in the sense that optimal microstructures are found that yield a targeted macroscopic property (in this case, NTE behavior).

In previous work,[11,12] we investigated whether isotropic potentials could be found that produce as ground states low-coordinate crystal structures (e.g., the honeycomb lattice in two dimensions and the diamond lattice) using inverse optimization methodologies. Here, we propose a solution to a different inverse problem: finding an isotropic pair potential that produces a classical many-particle system in a maximally coordinated, single-component crystalline state that undergoes NTE under a wide temperature and pressure range (including zero pressure). This is a counterintuitive proposition because conventional wisdom suggests that open structures composed of particles with highly directional interactions are necessary to observe NTE. Nonetheless, there is no fundamental reason for excluding this phenomenon in highly coordinated isotropic systems. Colloidal dispersions are a possible experimental test-bed system for NTE behavior, as in these systems interparticle interaction potentials may be designed by combining several interaction types (e.g., electrostatic repulsion, depletion, and dispersion).[13] Although the potential proposed in this paper is not explicitly constructed

† Part of the "Giacinto Scoles Festschrift".
* Corresponding author.
‡ Department of Physics.
§ Department of Chemistry.
|| Program in Applied and Computational Mathematics and PRISM.
⊥ Princeton Center for Theoretical Physics.

10.1021/jp076859l CCC: $37.00
Published on Web 11/08/2007

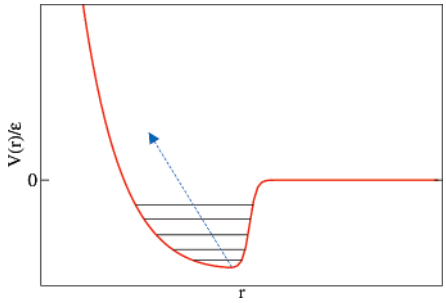

Figure 1. Schematic depiction of an isotropic pair interaction with a softened interior in its basin of attraction. Thermal fluctuations cause the average nearest-neighbor distance to decrease, resulting in an overall contraction of the system upon heating. Here, the horizontal black lines within the basin represent temperature values, and the broken line represents the thermally averaged nearest-neighbor distance.

from known colloidal interactions, it is possible that future developments will allow for such a potential to be devised.

We have found that a sufficient condition for a potential to give rise to a system with NTE behavior is that it exhibits a softened interior core within a basin of attraction (as depicted schematically in Figure 1). Such behavior of the potential may be characterized by its third derivative with respect to position at its minimum: if this is positive, the curvature is an increasing function of position, and the inner part of the basin is "softer" than the outer part. The potential function proposed in this paper thus belongs to a class of functions that give rise to NTE behavior; it will henceforth be called the softened-interior-core, or "SIC" potential. It is constructed by using a type of optimization procedure wherein parameters are chosen such that the potential will give rise to strong NTE behavior (via a large, positive third derivative of the pair potential with respect to r, the distance between particles). As will be explained in the next section, as the temperature is increased in such systems, the nearest-neighbor distances fluctuate about smaller average distances, causing NTE behavior. To demonstrate this phenomenon, we perform Gibbs-ensemble (constant number of particles, temperature, and pressure, or "NPT") Monte Carlo[14] simulations in both two and three dimensions in which the volume of the system is computed as a function of both ambient temperature and pressure. We find that, at low temperature, the system has its strongest negative thermal expansion. As the temperature is increased, the system contracts further until it reaches a minimum in volume (or area) and then expands as a function of temperature before melting. As a basis for comparison, we perform similar calculations using the Lennard-Jones potential, which exhibits conventional behavior in that it only expands as temperature is increased.

In section II, we discuss how the SIC potential was constructed. In section III, we discuss the details and results of the energetics calculations and NPT simulations, both for the SIC potential and for the Lennard-Jones potential. In section IV, we summarize the results and discuss future work pertaining to inverse problems in many-particle systems.

II. Theoretical Background

We consider classical N-particle systems (in two and three dimensions) with interactions that are pairwise additive and isotropic. Denoting the positions of the particles by $r_1, ..., r_N$ and their momenta by $p_1, ..., p_N$, the Hamiltonian of the system is

$$H(r_1, ..., r_N, p_1, ..., p_N) = \sum_{i<j}^{N} V_I(|r_i - r_j|) + \sum_{i=1}^{N} \frac{p_i^2}{2m} \quad (1)$$

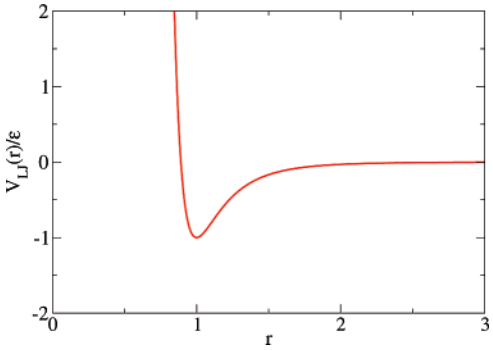

Figure 2. Lennard-Jones potential, as given in eq 3, with $\epsilon_{LJ} = \epsilon$ and $\sigma_{LJ} = 1/2^{1/6}$. As can be easily seen, the curvature of the potential is greater to the left of the minimum at $r = 1$ than to the right. As a result, when the temperature of a system interacting via this potential is increased, thermal fluctuations cause the average nearest-neighbor distance to increase.

where V_I is a interaction potential that is a purely radial function, and m is the mass of each particle, taken as unity for the remainder of this paper. Henceforth, we employ the reduced temperature of the system, $T^* = k_B T/\epsilon$, where T is the temperature, k_B is Boltzmann's constant, and ϵ is a parameter in the pair potential with units of energy.

The isobaric thermal expansion coefficient α is defined as

$$\alpha = \frac{1}{V}\left(\frac{\partial V}{\partial T}\right)_p \quad (2)$$

where V is the volume of the system, and p is pressure. Of course, α is negative if the system contracts upon heating. We seek an interaction potential that gives rise to this effect in an equilibrium sense.

A. Construction of the SIC Potential. In order to motivate how we devise a pair interaction potential that gives rise to negative thermal expansion for two- and three-dimensional many-particle systems in thermal equilibrium, consider first the Lennard-Jones potential:

$$V_{LJ}(r) = 4\epsilon_{LJ}\left[\left(\frac{\sigma_{LJ}}{r}\right)^{12} - \left(\frac{\sigma_{LJ}}{r}\right)^{6}\right] \quad (3)$$

where $\epsilon_{LJ} > 0$ and $\sigma_{LJ} > 0$ are energy and length parameters, respectively. This potential is shown in Figure 2, with $\epsilon_{LJ} = \epsilon$ and $\sigma_{LJ} = 1/2^{1/6}$. We adopt this parameter choice for the Lennard-Jones potential for the remainder of this paper. For a system of N particles interacting via the Lennard-Jones potential, where both the temperature and the pressure are zero, the equilibrium configuration in two dimensions is the triangular lattice, and in three dimensions, it is a maximally coordinated lattice (the hexagonal close-packed or hcp) with the nearest neighbors lying within the basin of attraction of the potential. Clearly, the curvature of the potential to the left of the minimum at $r = 1$ is significantly greater than that to the right. This is reflected in the negative third derivative of the potential at its minimum, that is, $V_{LJ}^{(3)}(1) = -1512\epsilon$. As a result, as the temperature is increased from zero, thermal fluctuations cause the distribution of nearest-neighbor distances to be skewed to the right. Thus, in thermal equilibrium, the particles are farther apart on average, and so the system should expand upon a temperature increase, that is, $\alpha > 0$. The behavior of the system should not qualitatively change if the pressure is positive. This is the mechanism for positive thermal expansion in this system.

Here, we construct an isotropic pair potential with a softened interior by finding a function with a strongly positive third

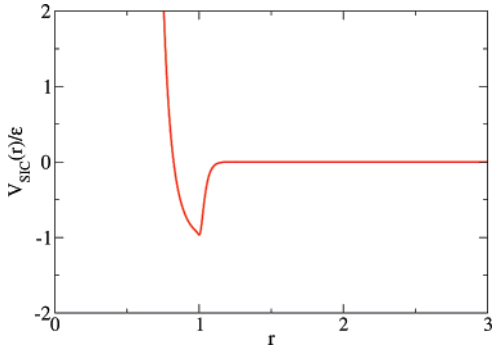

Figure 3. SIC potential, as given in eq 6, with the parameters $A = 9.30865$, $B = 0.1$, $C = 9A$, $r_M = 1$, $\epsilon_M = \epsilon$, and $\sigma_M = 0.5$. As can easily be seen, the curvature of the potential is greater to the right of the minimum at $r = 1.00069$ than to the left. As a result, when the temperature of a system interacting via this potential is increased, thermal fluctuations cause the average nearest-neighbor distance to decrease.

derivative (i.e., increasing curvature) within a basin of attraction (which should result in NTE behavior, as described in section I). We choose the Morse potential as a starting point, which is given by

$$V_M(r) = \epsilon_M\{\exp[2(r_M - r)/\sigma_M] - 2\exp[(r_M - r)/\sigma_M]\} \quad (4)$$

where $r_M > 0$ and $\sigma_M > 0$ are adjustable parameters. It has a basin of attraction with a minimum at r_M, and its third derivative evaluated at its minimum is negative; that is, $V_M^{(3)}(r_M) = -6\epsilon_M/\sigma_M^3$. Since we seek a potential with a positive third derivative in its basin, modification of this potential is necessary. We thus use a rescaling function for distance defined by

$$r^*(r) = Ar + B\{\log\cosh[C(r - r_M)] - \log\cosh(Cr_M)\} \quad (5)$$

where $A > 0$, $B > 0$, and $C > 0$ are free parameters such that $A - BC > 0$. This function has the property that for $r < r_M$, it asymptotes to a straight line going through the origin with slope $A - BC$, but for $r > r_M$, it quickly asymptotes to a straight line of slope $A + BC$. We define the softened-interior-core (SIC) potential to be

$$V_{SIC}(r) = \epsilon_M\left(\frac{0.8}{r}\right)^{15} + V_M(r^*(r)) \quad (6)$$

This potential is plotted in Figure 3 with $A = 9.30865$, $B = 0.1$, $C = 9A$, $r_M = 1$, $\epsilon_M = \epsilon$, and $\sigma_M = 0.5$. With this choice of parameters, the function is such that its curvature is greater to the right of its minimum, at $r = 1.00069$, than to the left, and it has a third derivative of $V_{SIC}^{(3)}(r_M) = 1.13660 \times 10^5\epsilon_M$. Note that the parameter values have been chosen such that this third derivative is quite large, with the intention of producing strong NTE behavior. In this sense, optimization of the potential is performed over the space of functions defined by eqs 5 and 6. The first term on the right side in eq 6 yields a stiffer core than what would otherwise have been present. As we show in section III.A., this has the effect of causing a maximally coordinated structure (face-centered cubic or fcc) to be the energetically stable structure at zero pressure. This ensures that the nearest neighbor is located near the bottom of the potential well. Farther neighbors interact only very weakly. Because of the softened interior within the basin of attraction of the SIC potential, given in eq 6, thermal fluctuations cause nearest-neighbor distances to decrease, on average. This has the effect of causing an overall contraction of the system. Note that this argument is independent of whether the system in question is two or three-dimensional. Thus, we expect the same potential (eq 6) to yield NTE behavior in both dimensions.

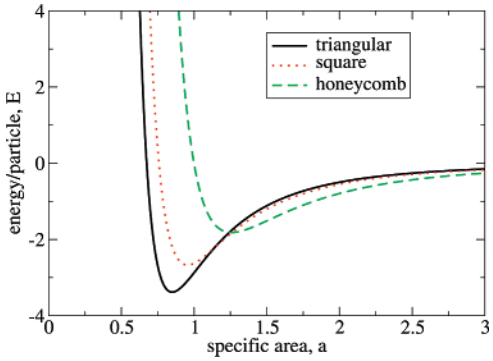

Figure 4. Two-dimensional lattice sums for the Lennard-Jones potential including the triangular, square, and honeycomb lattices. The lowest overall energy stucture is the triangular lattice, which is thus the stable structure at zero pressure. From the Maxwell construction, we find that the pressure range of stability at zero temperature is $0 < p < \infty$, and the range of stability in specific area is $0 < a < 0.85$.

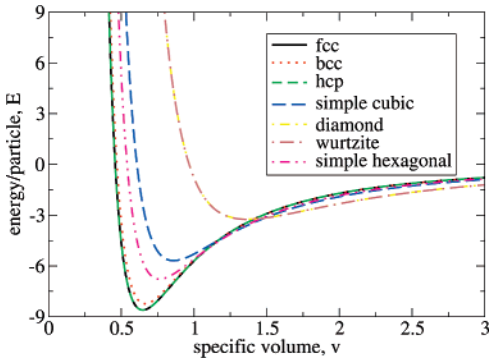

Figure 5. Three-dimensional lattice sums for the Lennard-Jones potential including the fcc, bcc, hcp, simple cubic, diamond, wurtzite, and simple hexagonal lattices. The lowest overall energy stucture is the hcp lattice, which is thus the stable structure at zero pressure. From the Maxwell construction, we find that the pressure range of stability at zero temperature is $0 < p < 1240$, and the range of stability in specific area is $0.33 < v < 0.65$.

This rescaling procedure could have been applied to the Lennard-Jones potential rather than the Morse potential. However, it was found that since the former possesses a much more strongly negative third derivative at its minimum than the latter (when their minima are at the same position and depth), the Morse potential is more suitable for exhibiting a strongly increasing curvature within its attractive basin.

III. Results and Discussion

In this section, we present lattice sums (Madelung energies as a function of specific area or volume for a number of crystal structures), for the Lennard-Jones and SIC potential systems in two and three dimensions. We thus determine the low temperature thermodynamically stable crystal structure for each, and using the Maxwell construction,[15] we ascertain the zero-temperature range of stability in pressure. In this section, we take $\epsilon = 1$.

A. Energetics of the Lennard-Jones and SIC Potential. The lattice sums for the Lennard-Jones systems in two and three dimensions are shown in Figures 4 and 5, respectively. In the two-dimensional case, the Madelung energies of three crystal structures (the triangular lattice, square lattice, and honeycomb lattice) are plotted as a function of specific area, a. The lowest

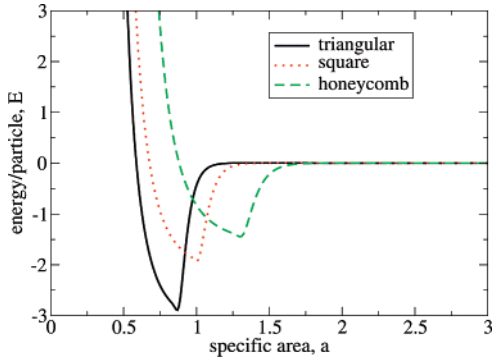

Figure 6. Two-dimensional lattice sums for the SIC potential including the triangular, square, and honeycomb lattices. The lowest overall energy structure is the triangular lattice, which is thus the stable structure at zero pressure. From the Maxwell construction, we find that the pressure range of stability at zero temperature is $0 < p < \infty$, and the range of stability in specific area is $0 < a < 0.87$.

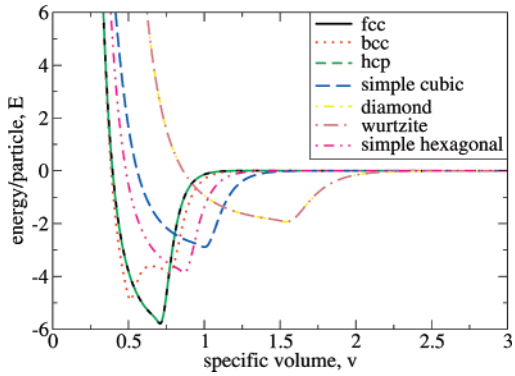

Figure 7. Three-dimensional lattice sums for the SIC potential including the fcc, bcc, hcp, simple cubic, diamond, wurtzite, and simple hexagonal lattices. The lowest overall energy stucture is the hcp lattice, which is thus the stable structure at zero pressure. From the Maxwell construction, we find that the pressure range of stability at zero temperature is $0 < p < 4.5$, and the range of stability in specific area is $0.70 < v < 0.71$. There is another region of stability of this system at significantly smaller specific volume, but this is irrelevant to the present work.

overall energy stucture is the triangular lattice, which is thus the most stable structure at zero pressure. From the Maxwell construction, we find that the pressure range of stability at zero temperature is $0 < p < \infty$, and the range of stability in specific area is $0 < a < 0.85$. The lattice sums for the three-dimensional system are plotted in Figure 5, with the Madelung energies of seven crystals being plotted (fcc, body-centered cubic (bcc), hcp, simple cubic, diamond, wurtzite, and simple hexagonal lattices). The maximally coordinated structures, namely, fcc and hcp, clearly have the lowest energies overall and are thus the stable structures at zero pressure. These two lattices are extremely close in energy, although the hcp has the lower energy for specific areas for which the nearest neighbor is near the bottom of the basin of attraction, which is the regime we study in this paper. Its pressure range of stability at zero temperature is $0 < p < 1240$, and its range of stability in specific volume is $0.33 < v < 0.65$. Lattice sums for the SIC potential systems in two and three dimensions (with parameters $A = 9.30865$, $B = 0.1$, $C = 9A$, $r_M = 1$, $\epsilon_M = \epsilon$, and $\sigma_M = 0.5$) are shown in Figures 6 and 7. For both cases, the same lattices are plotted as in the Lennard-Jones case. As in the two-dimensional Lennard-Jones system, the triangular lattice has the lowest overall energy and is thus the zero-pressure stable structure. The pressure range of stability at zero temperature is $0 < p < \infty$ and the range of stability in

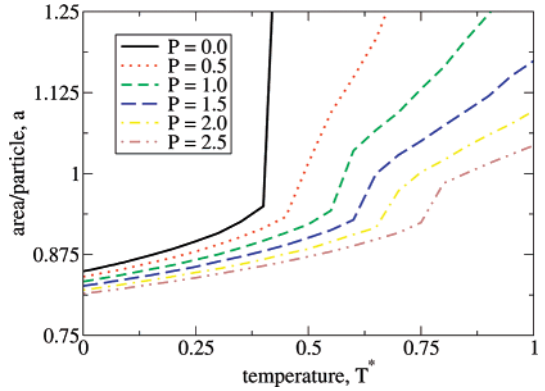

Figure 8. Specific area as a function of temperature for a number of different pressure values for the two-dimensional Lennard-Jones system. These results are obtained from NPT Monte Carlo simulations with $N = 1040$ particles and periodic boundary conditions. In its crystalline (triangular) state, this system expands when temperature is increased for all pressures and temperatures. Note that kinks in the curves indicate melting of the crystal.

specific area is $0 < a < 0.87$. In the three-dimensional SIC system, the maximally coordinated structures are again the most stable and extremely close in energy. However, in this case, it is the fcc lattice which has the lowest overall energy. Note that the stiff-core term in the potential V_{SIC}, the first term on the right-hand side of eq 6, is essential for the maximally coordinated structures to have lower energies than the other lattices. Without this term, lower-coordinated structures are energetically stable at specific volumes for which several neighbor distances may fall within the basin of attraction of the potential. It follows that the argument made in section II.A motivating construction of the SIC potential as a candidate for NTE behavior would not hold in this case.

In three dimensions, there are two distinct pressure and density regions in which the fcc lattice is stable; however, we are only interested in the one in which the nearest neighbor falls within the basin of attraction of the potential. For this region, the pressure range of stability at zero temperature of the fcc lattice in the three-dimensional case is $0 < p < 4.5$, and the specific volume range of stability is $0.70 < v < 0.71$.

B. NPT Monte Carlo Simulation Results. Monte Carlo simulations were run in the NPT ensemble on the two- and three-dimensional Lennard-Jones and SIC systems for a number of pressures and temperatures. In all simulations, Monte Carlo sampling is carried out until equilibrium is achieved, after which the fluctuating area/volume is repeatedly sampled until a sufficiently precise average is obtained. In both two-dimensional systems, the triangular lattice was used with $N = 1020$ particles in a rectangular simulation cell with periodic boundary conditions imposed. In both three-dimensional systems, the fcc lattice was used with $N = 864$ in a cubic cell also with periodic boundary conditions. Note that in the case of the Lennard-Jones system, the hcp, not the fcc, lattice is the thermodynamically stable structure. However, we employ the latter in simulations in order to directly compare the results to those of the SIC system. This choice is justified because of the extreme closeness in Madelung energies of the fcc and hcp lattices. To confirm that the maximally coordinated lattices were indeed the ground states for each of the four systems discussed here, annealing simulations were performed in which each system was cooled through its freezing point. In each case, a maximally coordinated lattice resulted as the appropriate equilibrium crystal state.

The area/volume dependence on temperature of the Lennard-Jones systems in two and three dimensions is shown in Figures

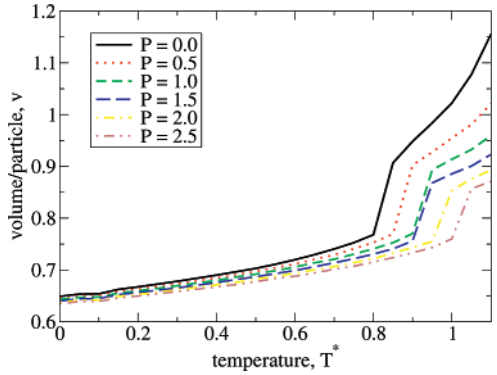

Figure 9. Specific volume as a function of temperature for a number of different pressure values for the three-dimensional Lennard-Jones system. These results are obtained from NPT Monte Carlo simulations with $N = 864$ particles and periodic boundary conditions. In its crystalline (fcc) state, this system expands when temperature is increased for all pressures and temperatures. Note that the "kinks" in the curves indicate melting of the crystal.

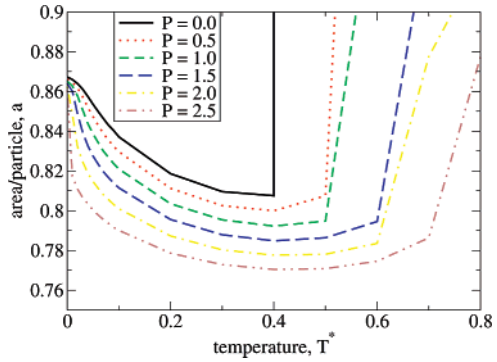

Figure 10. Specific area as a function of temperature for a number of different pressure values for the two-dimensional SIC system. These results are obtained from NPT Monte Carlo simulations with $N = 1040$ particles and periodic boundary conditions. In its crystalline (triangular) state, this system undergoes NTE for low temperatures, but as temperature is increased, thermal expansion passes through zero and then becomes positive. Note that the "kinks" in the curves indicate melting of the crystal.

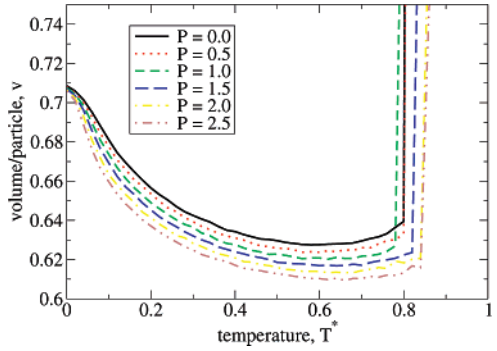

Figure 11. Specific volume as a function of temperature for a number of different pressure values for the three-dimensional SIC system. These results are obtained from NPT Monte Carlo simulations with $N = 864$ particles and periodic boundary conditions. In its crystalline (fcc) state, this system undergoes NTE for low temperatures, but as temperature is increased, thermal expansion passes through zero and then becomes positive. Note that the "kinks" in the curves indicate melting of the crystal.

8 and 9, respectively. The plots show results for a number of pressure values, $p = 0$, 0.5, 1.0, 1.5, 2.0, and 2.5. The data show that, in both cases, the solid expands until it melts. The sharp bends or "kinks" in the curves indicate the first-order melting transition.

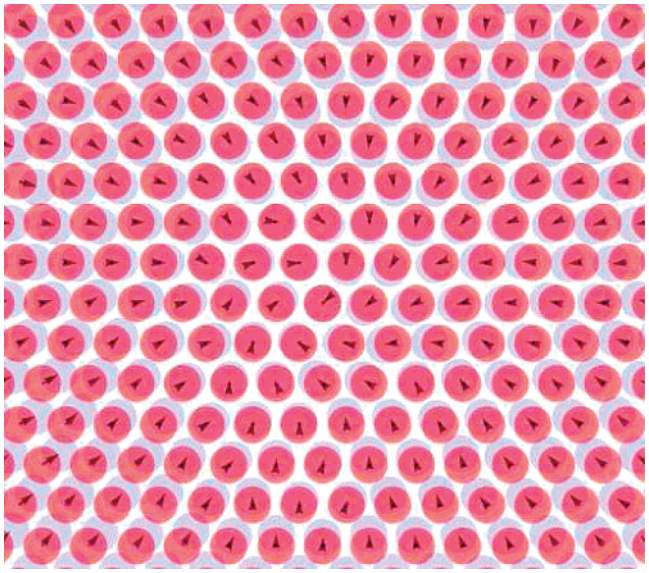

Figure 12. Section of two configurations of the SIC system, one at $T^* = 0.0$ (dark) and the other at $T^* = 0.3$ (light). The configurations are snapshots taken from NPT Monte Carlo simulations. Arrows indicate the displacement of the particles upon heating from the former temperature to the latter. The ambient pressure is $p = 1.0$. The system appears to undergo a simple rescaling.

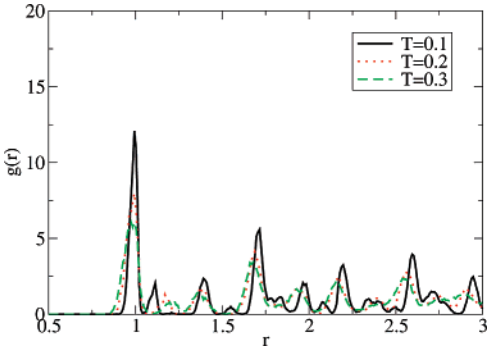

Figure 13. Radial distribution function for the SIC system in three dimensions at $p = 1.0$ for three temperatures, $T^* = 0.1$, 0.2, and 0.3. As a result of the increasing curvature of the SIC potential, given in eq 6, near its minimum, the first peak is increasingly skewed to smaller r as the temperature is increased. The second peak is not present in the perfect fcc lattice and represents a shearing of the system.

Simulation results for the SIC potential systems in two and three dimensions (with parameter values $A = 9.30865$, $B = 0.1$, $C = 9A$, $r_M = 1$, $\epsilon_M = \epsilon$, and $\sigma_M = 0.5$) are shown in Figures 10 and 11, respectively. The data show that for low temperature and for each pressure value (among $p = 0$, 0.5, 1.0, 1.5, 2.0, and 2.5), in both two and three dimensions, the system contracts. At a certain pressure-dependent temperature, the thermal expansion coefficent passes through zero and becomes positive (at the minima of the curves). At higher temperatures, the system undergoes positive thermal expansion until it melts. The temperature at which zero thermal expansion is achieved is an increasing function of the pressure.

For the two-dimensional SIC system, we show in Figure 12 two configurations of the system at temperatures $T^* = 0.0$ and $T^* = 0.3$, with both at pressure $p = 1.0$. Arrows show the direction that the particles move when the temperature is increased from $T^* = 0.0$ to $T^* = 0.3$.

The radial distribution function, $g(r)$, is plotted for the three-dimensional case in Figure 13, for pressure $p = 1.0$ and temperatures $T^* = 0.1$, 0.2, and 0.3. While the first peak (near $r = 1$) appears to reach its maximum at nearly the same distance

for each temperature, the left tail of the first peak extends further and further to the left as temperature is increased. This is an indicator of the NTE mechanism of the system. Here, thermal fluctuations cause the nearest-neighbor distance distribution to widen, but the increasing curvature as r increases of the potential, V_{SIC}, causes this distribution to be skewed toward lower r. The average volume of the system decreases as a result. Note that this is exactly the mechanism of negative thermal expansion in the two-dimensional SIC system as well. Figure 13 also shows an anomalous second peak not present in the radial distribution function of the fcc lattice. This indicates that in additon to the volume change, the system undergoes a shearing as temperature is increased from zero.

IV. Conclusions

In this paper, we have proposed an isotropic pair interaction potential for a system of classically interacting particles that gives rise to negative thermal expansion in maximally coordinated lattices in both two and three dimensions. Previously, this phenomenon had only been observed in low-density open crystals[1] and in three-component composites.[3] The key feature of the proposed potential, $V_{SIC}(r)$, which is based on a modification of the Morse potential, is a basin of attraction wherein the curvature is an increasing function of r. With this property, thermal fluctuations cause the nearest-neighbor distances in the maximally coordinated lattices to decrease on average, resulting in an overall contraction.

Using NPT Monte Carlo simulations, we compared the behavior of systems interacting via $V_{SIC}(r)$ to those interacting via the standard Lennard-Jones interaction potential. We found that NTE remained present for the former over a large temperature and pressure range, with zero pressure included in the latter. At sufficiently high temperatures (still below the melting point), the thermal expansion coefficent goes to zero and then becomes positive. The proposed potential may be seen as a possible solution to an inverse problem: that of finding a microscopic interaction that yields a desired macroscopic property. Indeed, by adjusting the parameters of the Morse potential, given in eq 4 and in the rescaling function given in eq 5, the thermal expansion coefficient may be manipulated.

In future work, we aim to continue the inverse problem program of finding isotropic interaction potentials that yield systems with targeted material properties. One example of such a problem is finding isotropic potentials that favor disordered systems as well as certain types of defects in crystalline solids. Another example is the problem of designing an isotropic interaction potential that yields a material with negative Poisson ratio, that is, wherein compression in one direction causes compression in the orthogonal direction. This effect has been studied experimentally and theoretically in composite materials,[16] in foam structures,[17,18] and in atomic solids.[19] Another challenging open problem is to find an isotropic pair potential that produces a substance that contracts upon melting and then continues to contract over some temperature range (as is the case in water). Last, there is the challenge of designing an isotropic pair potential that yields a system that freezes into a crystalline state upon an increase in temperature ("inverse melting"), over a wide temperature and pressure range. Both isotopes of helium exhibit this property,[20,21] and simulations have shown that a modified Gaussian−core interaction does as well.[22] This counterintuitive behavior is of fundamental interest because it challenges the conventional wisdom of equilibrium fluid−solid phase transitions.

Acknowledgment. This work was supported by the Office of Basic Energy Sciences, U.S. Department of Energy, under Grant DE-FG02-04-ER46108. M.C.R. acknolwedges the support of the Natural Sciences and Engineering Research Council of Canada.

References and Notes

(1) Evans, J. S. O. *J. Chem. Soc., Dalton Trans.* **1999**, *19*, 3317.
(2) Pryde, A. K. A.; Hammonds, K. D.; Dove, M. T.; Heine, V.; Gale, J. D.; Warren, M. C. *J. Phys.: Condens. Matter* **1996**, *8*, 973.
(3) Sigmund, O.; Torquato, S. *Appl. Phys. Lett.* **1996**, *69*, 3203; Sigmund, O.; Torquato, S. *J. Mech. Phys. Solids* **1997**, *45*, 1037; Gibiansky, L. V.; Torquato, S. *J. Mech. Phys. Solids* **1997**, *45*, 1223.
(4) Fletcher, N. H. *The Chemical Physics of Ice*; Cambridge University Press: Cambridge, 1970.
(5) Note that liquid water also undergoes NTE in the temperature range 0 °C < T < 4 °C;[1] however, this is not germane to the present work since our focus here is NTE behavior in the crystalline state.
(6) Ashcroft, N. W.; Mermin, N. D. *Solid State Physics*; Saunders College: Philadelphia, PA, 1976.
(7) Mary, T. A.; Evans, J. S. O.; Vogt, T.; Sleight, A. W. *Science* **1996**, *272*, 90.
(8) Forster, P. M.; Yokochi, A.; Honig, A. J. W. M. *J. Solid State Chem.* **1998**, *140*, 157.
(9) Biernacki, S.; Scheffler, M. *Phys. Rev. Lett.* **1989**, *63*, 290.
(10) Evans, J. S. O.; Mary, T. A.; Sleight, A. W. *J. Solid State Chem.* **1998**, *137*, 148.
(11) Rechtsman, M. C.; Stillinger, F. H.; Torquato, S. *Phys. Rev. Lett.* **2005**, *95*, 228301.
(12) Rechtsman, M. C.; Stillinger, F. H.; Torquato, S. *Phys. Rev. E* **2007**, *75*, 31403.
(13) Russel, W. B.; Saville, D. A.; Schowalter, W. R. *Colloidal Dispersions*; Cambridge University Press: Cambridge, 1992.
(14) Frenkel, D.; Smit, B. *Understanding Molecular Simulation*; Academic Press, Inc.: Orlando, FL, 2001.
(15) Landau, L. D.; Lifshitz, E. M. *Statistical Physics*; Butterworth−Heineman: Oxford, 2000.
(16) Xu, B.; Arias, F.; Brittain, S. T.; Zhao, X.-M.; Grzybowski, B.; Torquato, S.; Whitesides, G. M. *Adv. Mater.* **1999**, *11*, 1186.
(17) Lakes, R. S. *Science* **1987**, *235*, 1038.
(18) Friis, E. A.; Lakes, R. S.; Park, J. B. *J. Mater. Sci.* **1988**, *23*, 4406.
(19) Keskar, N. R.; Chelikowsky, J. R. *Nature* **1992**, *358*, 222.
(20) Dobbs, E. R.; Hallock, R. B. *Phys. Today* **2002**, 55.
(21) Wilks, J.; Fairbank, H. A. *Am. J. Phys.* **1968**, *36*, 764.
(22) Feeney, M. R.; Debenedetti, P. G.; Stillinger, F. H. *J. Chem. Phys.* **2003**, *119*, 4582.